https://dx.doi.org/10.1016/j.sna.2019.111745

Design and verification of a wireless sensing system for monitoring large-range ground movement

Chuncheng Yao[a], Chengyu Hong[a,*], Dong Su[a], Yifan Zhang[b], Zhenyu Yin[c]

[a] College of Civil and Transportation Engineering, Shenzhen University

[b] University Research Facility in 3D Printing, The Hong Kong Polytechnic University, Hung Hum, Kowloon, Hong Kong, China

[c] Department of Civil and Environmental Engineering, The Hong Kong Polytechnic University

Abstract

In this study, flex sensors and Bluetooth wireless transmission technology were combined to fabricate a wireless sensing system for monitoring ground movement. A typical hinge joint structure was designed and fabricated to embed flex sensors. A number of these typical hinge joint elements were used to measure distributed ground movement. Calibration tests show that minimum resolution, sensitivity, and measurement range of flex sensors were 0.5°, 2.0~2.3 count/° and -30°~+70°, respectively. In experimental study, five flex sensors were placed inside a slope model for both soil settlement and horizontal displacement measurement. Calculated settlement of the data measured from flex sensors were verified with the output data of Linear Variable Displacement Transducer (LVDT), and the obtained maximum errors were less than 0.5 mm when the maximum ground displacement was approached. Besides, the calulated horizontal soil displacement from measurement of flex sensors has proved that flex sensors can be applied for monitoring soil movement when large ground deformation occurs.

Keywords: Flex sensors, Bluetooth, soil movement, large ground deformation

1. Introduction

A large number of researches focusing on the application of flex sensors in human machine interface devices, rehabilitation investigation and security sensing systems have been performed these years [1]–[7]. For instance, the sensors have been placed on the user's skin within singular sleeves [8], or inserted in an open wearable architecture [9], or embedded into clothes [10], [11], or deposited onto textile fibers [12], or even directly utilized as a sort of skin themselves [13]. Flex sensors were used to interpret sign language by mounting them on gloves and interfacing with signal processing circuits [14]-[16] as well.

Flex sensors have been widely used to reflect bend movement. Strain and flex sensors have been applied in health monitoring to measure the muscle joint angle and movement [17]-[19]. Flex sensors can be used to measure knee angle movements [20] and finger bend movements [21]-[23]. By placing flex sensors at joint positions, the flex sensors can be used to monitor the damage e condition of different types of joints. However, limited studies have been reported using flex sensors to track internal ground movement.

There are some conventional instruments for monitoring ground movements. For instance, a global positioning system (GPS) can be used to measure ground surface movement by providing time-series of 3D topographical data [24]. Besides, a

conventional inclinometer system consists of a plastic casing that is installed in a near vertical position underground, with a servo-accelerometer or electro-level sensor inserted into the casing to measure the local tilt of the casing in response to ground movement [25]. However, this GPS has low measurement accuracy, and the inclinometer system has limitations, such as high cost, poor durability and reduced accuracy operating under steeply inclined conditions [25]. In addition, Fiber Bragg grating (FBG) is widely applied in the measurement of strain and temperature[26], [27]. For example, a FBG tilt sensor fabricated with fused deposition modeling method was proposed to measure tension and compression strain resulted from different tilt angles, which was used for monitoring the internal ground movement [28]. Though there are several tilt sensors proposed based on FBG sensors, and most of these tilt sensors have the characteristics of high accuracy, temperature independent, and small size [29]-[31], these s are fragile and wired in actual monitoring tests, which is inferior to flex sensor, which can be used over 1 million cycles and work under temperature range of -35~ +80°C.

This study proposes to use a flex sensor combined with Bluetooth wireless transmission technology for soil movement monitoring. A flex sensor is installed in a joint structure fabricated with a free joint and two sensing beams to measure ground movements from tilt angles. The flex sensor was used to monitoring the internal settlement and horizontal movement of a sandy slope model and compared with conventional displacement sensor for validation. The present flex sensor is characterized by a large number of typical advantages, such as ease of use, simple structural design, highly flexible senor component, and comfort of embedding in the soil for ground movement monitoring. Besides, it is stable in performance, continuous output of real-time data, and simple working principle.

2. Design and fabrication of flex sensors combined with Bluetooth wireless transmission technology

A flex sensor is a resistive sensor that converts physical energy into electrical energy. It has different resistance values at different bending angles. The amount of electrical signal output is used to reflect the bend angle change of the flex sensor. A layer of carbon/polymer ink is printed on substrate of flex sensor, and fine micro cracks present along the substrate. When bend angle of flex sensors increase, the micro cracks open and also increase, so that the overall conductivity of the sensor decreases, and the overall resistance increases.

Figure 1 shows basic structure of a flex sensor combined with Bluetooth wireless transmission technology. The flex sensor is an element, which is connected to a Bluetooth for data collection. A joint structure characterized by two sensing beams connected by a free joint was fabricated to measure the relative angle change α between the two beams as shown in Figure 1. Each time when the relative position between the two beams is changed, the flex sensor embedded inside the two beams will exhibit a corresponding single change, indicating the extent of bend angle change between the two beams. These flex sensors used in this study were purchased from market, and the

model of the sensors is FLEX Sensor 2.2", produced from company, Spectra Symbol. A total length of a sensing beam is 70 mm (the length can be changed for different tests) with a width of 10 mm and an external thickness of 5 mm. A small internal slot (7 mm in width, 1 mm in thickness, and the same length as sensing beam) was created inside each sensing beam for the placement of flex sensor. And the back side of flex sensor was bonded inside the slot with double-sided tape to make sure that the sensors just slide with no ripples during the bending. A steel bearing with a diameter of 5 mm is installed between the two beams for controlling and reflecting the relative rotation movement between two beams as shown in Figure 1. Finally, flex sensors will be placed inside a slope model for monitoring the tilt angle change after vertical load is applied on top surface of the slope model.

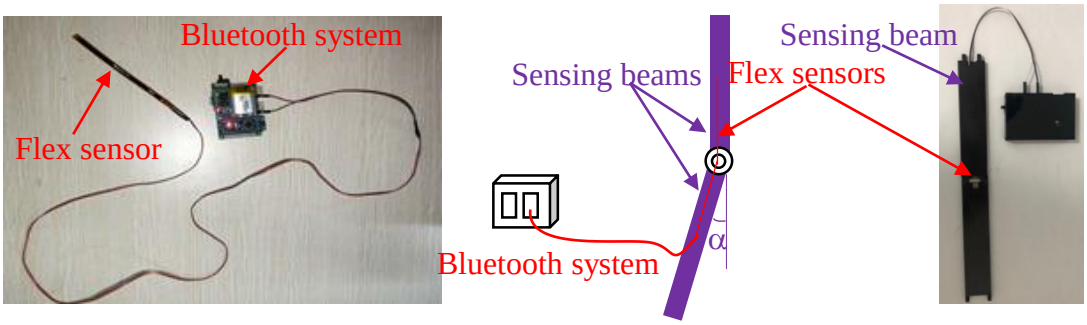

Figure 1 A wireless flex sensor connected to a Bluetooth data collection system

3. Calibration test of flex sensors

A total of five flex sensors were used for monitoring the internal tilt angle change of a slope model. These five sensors, namely A1~A5, were designed according to the designed schematic structure shown in Figure 1. The calibration test of the five flex sensors was carried out in a laboratory. A positive tilt angle was defined as the tilt angle of flex sensor rotating in a clockwise direction, as marked in Figure 1. The Bluetooth data collection system connected with a softeware, XCOMv2.0®, was used to collect all flex sensor data from Bluetooth wireless transmission technology.

A standard angle gauge was used to control the tilt angles of flex sensors with a measurement resolution of 0.1°. The sensing beams were fixed entirely on the angle gauge by a clamp. Inclination angle was applied on the beam step by step with an angle increment of 5°, which can be directly observed from the angle gauge. The response time of flex sensor is 0.2 s. The tilt angle range from the calibration test was -30°~+70°. Figure 2 depicts flex sensor reading of the five flex sensors against tilt angle from angle gauge. It is clear that the flex sensor readings are linearly proportional to the change of tilt angle. This linear relationship can be used to obtain the occurred tilt angle using flex sensors in applications. It should be noted that the minimum resolution and sensitivity of the flex sensors were around 0.5° and 2.0~2.3 count/°, respectively. Therefore, flex sensors can be used to monitor large tilt angles occurred inside ground.

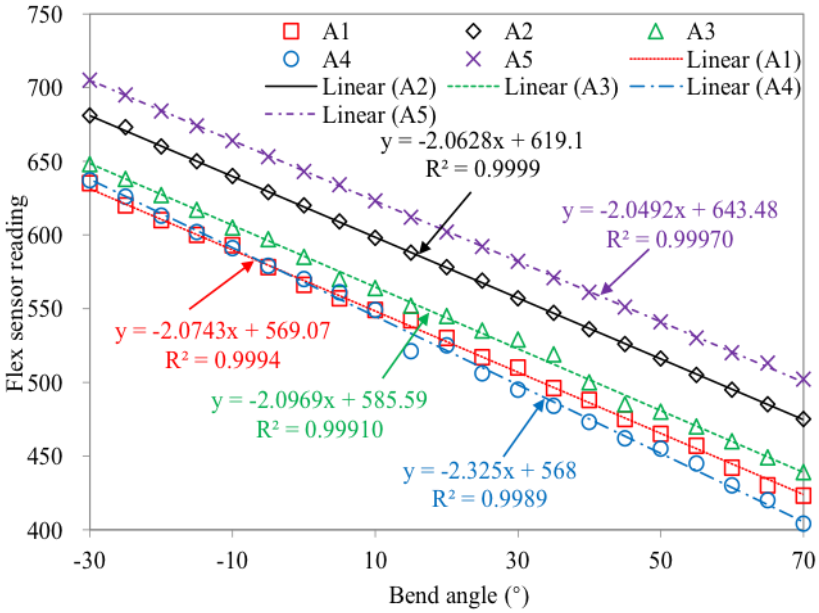

Figure 2 Calibration data of five flex sensors at different bend angles in calibration tests.

4. Hysteresis test and repeatability test for calibration of flex sensors

A hysteresis test of flex sensor was carried out. In the hysteresis test, the flex sensor was bended under angles of -30° and 30° for 100 times. Figure 3 presents the hysteresis test data. It is clear that the obtained relationship between flex sensor readings and bend angles are approximately linear.

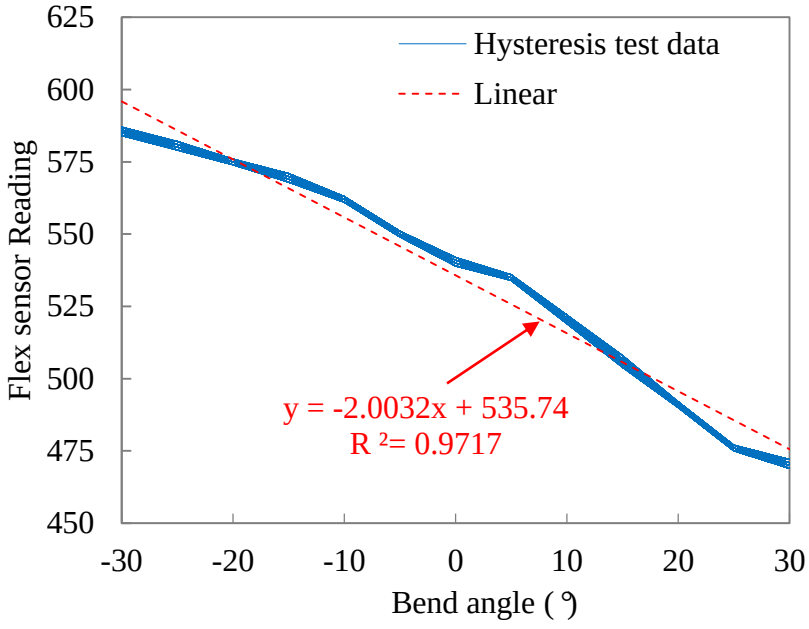

Figure 3 Hysteresis test data of a flex sensor.

Another flex sensor with sensing beams was fabricated. The calibration test of this flex sensor was conducted. Figure 4 describes the test result, and it presents the linearity between bend angle and flex sensor reading. Hence, the repeatability of

the calibration test results can be assured. This phenomenon may be due to that the bend position is a point on the flex senor rather than the whole sensor.

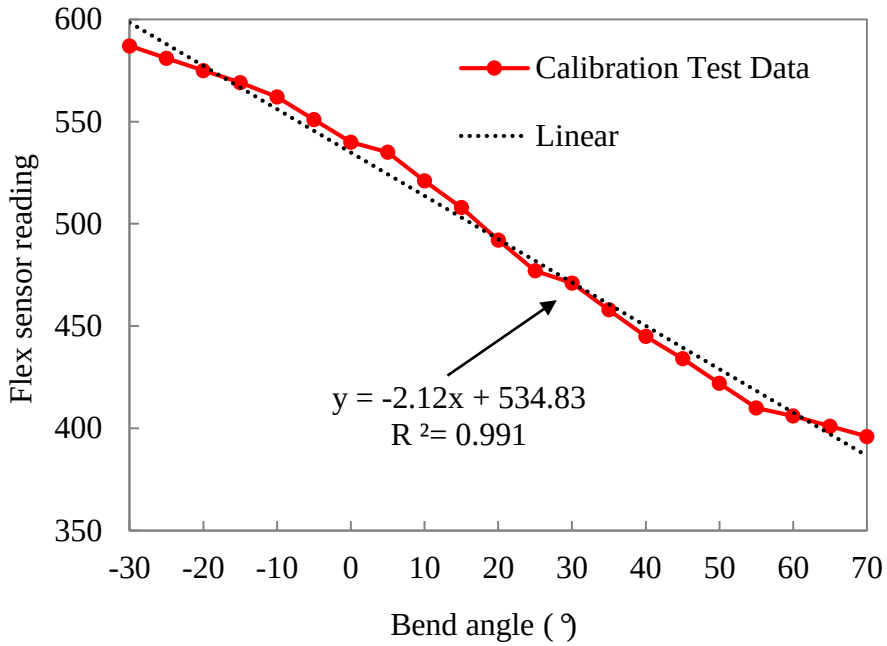

Figure 4 Repeatability test result of the calibration test results.

5. Monitoring test of a slope model

A sandy slope model was prepared in a laboratory instrumented with the new flex sensor array and the linear variable displacement transducer (LVDT) array, as shown in Figure 5. The measurement range and resolution of LVDT is 0~25mm and 0.0001mm, respectively. The sand material used in the test is medium coarse sand with an average unit weight of 17 kN/m^3 and internal friction angle of 32°. A model box with an inner dimension of 600×280×400 mm (length × width × height) was used to establish the sandy slope. The maximum height of the slope model was 330 mm, and the length and height of slope toe were 30 mm and 130 mm, respectively. Vertical loading test was carried out by continuously applying vertical load on the top surface of the slope at a velocity of 0.8 kN/min until slope collapse. The loading area was 3900 mm^{2,} with a corresponding loading rate of 205 kPa/min.

According to Figure 5, five flex sensors, namely A1, A2, A3, A4, and A5 were used to monitor the slope model in laboratory. The sensing structure for measuring ground settlement was anchored at the left edge of the model box, and the other one for monitoring horizontal movement was anchored at the bottom of the model box. Lengths of three sensing beams connecting A1 and A2 were 65, 105 and 105 mm, respectively; and, lengths of four sensing beams connecting A3, A4 and A5 were 75, 75, 75 and 40 mm, respectively. Flex sensor A1 was located at the distance of 65 mm from the left edge of the model box; flex sensor A2 was at the distance of 105 mm from A1; flex sensor A5 was placed at the distance of 40 mm from the bottom of the model box; and flex sensors A4 and A3 was located at the distances of 75 mm and 150 mm, respectively, from A5. There were three test points, namely T1, T2 and T3 as shown in, where were

installed with the traditional sensors, LVDTs. All LVDTs were perpendicular to the flex sensors mounted inside the slope model. LVDT B1 was at a distance of 117.5 mm from the left edge of the model box; LVDT B2 was at a distance of 157.5 mm from B1; and LVDT B3 was at a distance of 265 mm from the bottom of the model box. It is noted that the measurement range and resolution of LVDT are 0~25mm and 0.0001mm, respectively. The photos of the model slope installed with flex sensor array and LVDTs are as shown in Figure 6.

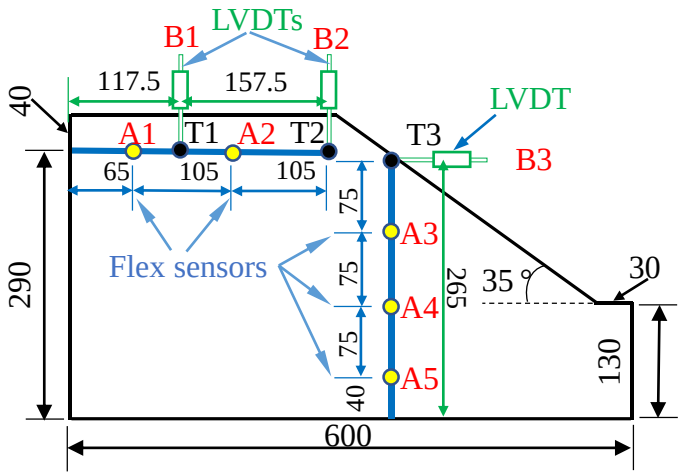

Figure 5 A schematic view of the slope model mounted with flex sensors and LVDTs (Unit: mm)

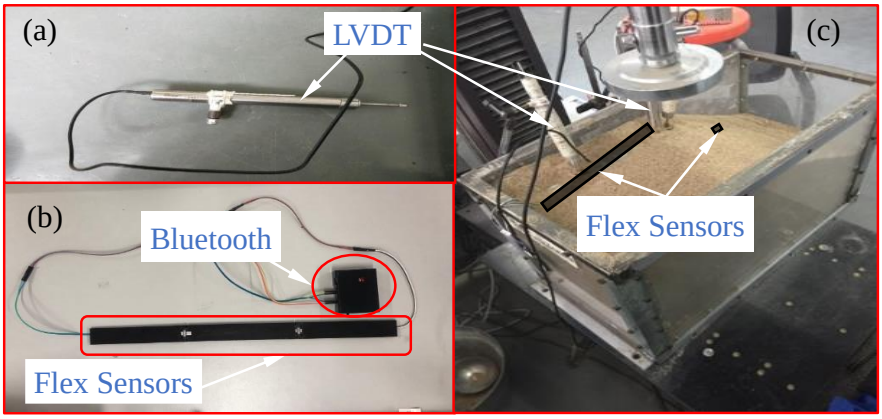

Figure 6 Photos of (a) LVDT, (b) Flex sensors combined with Bluetooth wireless transmission technology, (c) the model slope installed with flex sensors and LVDTS

6. Test data and analysis

6.1 Principle of data processing measured from flex sensors

Figure 7 (a) presents the initial sensing structure of flex sensors for monitoring ground movement, and Figure 7 (b) shows the structure of flex sensors with tilt angles. The obtained tilt angle of each sensing beam can be directly used to calculate soil settlement at different positions. Assuming the tilt angle of the n+1 sensing beams from left to the right are θ_1, θ_2,$\cdots$, θ_n, and length of each section is L_1, L_2, $\cdots$, L_n, respectively. When the test position of the sensing structure is l, where $l \in (\sum_1^i L_i, \sum_1^{i+1} L_{i+1})$, the ground movement ($S$) of the test position can be calculated as follows:

$$S = -\sum_{x=1}^{i-1}\left[\sin\left(\sum_{1}^{i-1}\theta_x\right)\times L_{x+1}\right] - \sin\left(\sum_{x=1}^{i}\theta_x\right)\times\left(l-\sum_{x=1}^{i}L_x\right) \quad (1)$$

where, x=1, 2,$\cdots i$. It is noted that negative settlement values indicate upward ground movement.

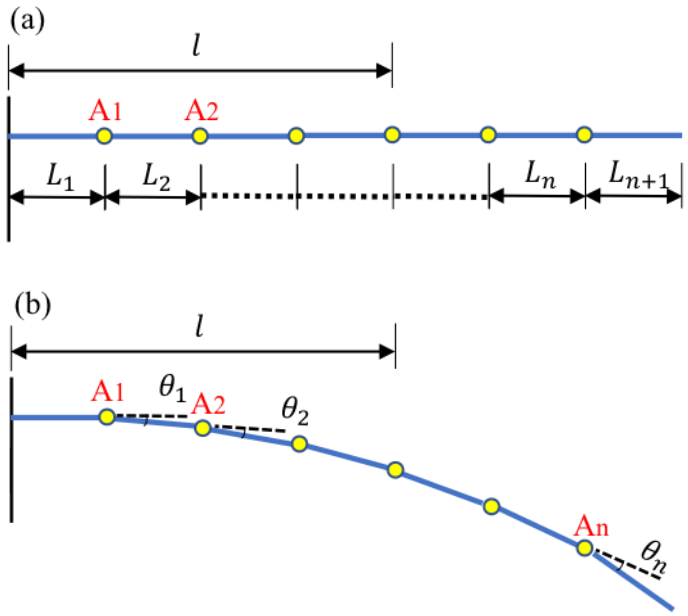

Figure 7 (a) The initial sensing structure of flex sensors
(b) A schematic diagram of ground movement calculation (unit: mm)

6.2 Settlement data and analysis

The data obtained by two flex sensors (A1 and A2) were processed to obtain the tilt angle against time by using a calibration relationship from the calibration test. Relationships of tilt angle changes of the two sensors against elapsed time during loading test of the slope model are presented in Figure 8. When the tilt angle value was positive, the flex sensor was clockwise bended concerning the initial plane. The measured tilt angle value of flex sensor, A1, increases smoothly in general, approaching maximum tilt angles of around 3°, while the measured tilt angle value shows a smooth fall, approaching minimum tilt angles of around -1.5° for flex sensor, A2.

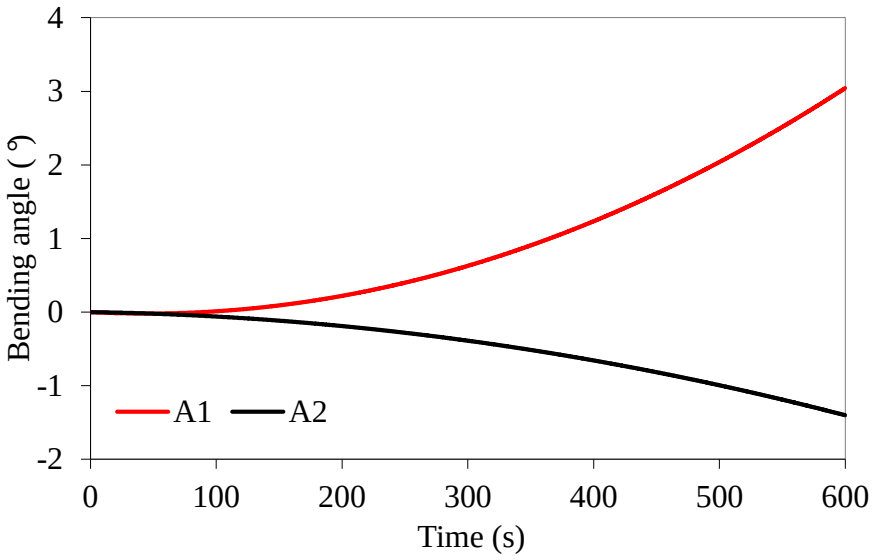

Figure 8 Tilt angle against time processed from measured data of two flex sensors

The settlements of test points (T1 and T2) calculated from the data measured from flex sensors were named as S_1 and S_2, respectively. The schematic diagram of the settlement calculation for these flex sensors is converted from Figure 7, and the detailed information is as shown in Figure 9. All dimension values are marked in Figure 9 for better identification of all sensor positions.

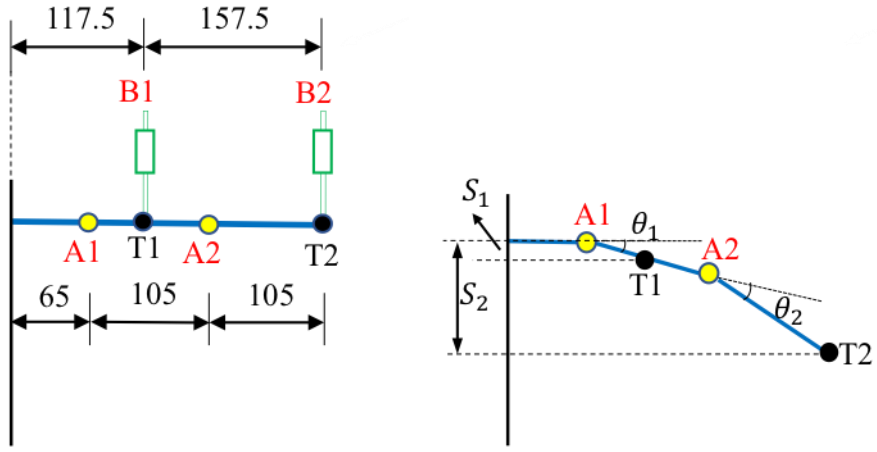

(a) (b)

Figure 9 (a) The initial sensing structure of flex sensors,
(b) A schematic diagram of settlement calculation (unit: mm)

Assuming the tilt angle of the two flex sensors from left to the right of the sensing beams are θ_1 and θ_2, respectively, then a settlement of each test point (T1 and T2 respectively) can be calculated according to Eq. (1), combined with the data of relative position depicted in Figure 9.

Figure 10 presents the calculated ground settlement data monitored from flex sensors and the settlement values measured from LVDTs. With the load increases, the settlement of test points, T1 and T2, measured from two LVDTs decreased

monotonically, and the amount of settlement on the measuring point of T2 was smaller compared with T1. The settlement values of T1 and T2 were -2.6 mm and -8.3 mm, respectively, when the test time was 600s. It is also clear that the relationships between settlement and time of the test points measured from flex sensors are entirely consistent with the settlement data from LVDTs. The settlement calculated from flex sensors decrease quickly against elapsed time with the maximum settlement of -2.8 mm and -8.6 mm for the test points of T1 and T2, respectively. It could also be found that the absolute value of the maximum settlement error of test point T1 between flex sensors and LVDT is around 0.3 mm, and the absolute value of maximum settlement error between FSS and LVDT is approximately 0.5 mm. But with the load decreases, the absolute value of tilt angle of flex sensor increases, the settlements measured from flex sensors are more close to the measurement data from LVDTs. It is also found that the settlement error of test point T1 between flex sensors and LVDT is around -0.2 mm at 600 s, and the settlement error between flex sensors and LVDT is around -0.3 mm at 600 s, indicating that flex sensors have reliable monitoring performance.

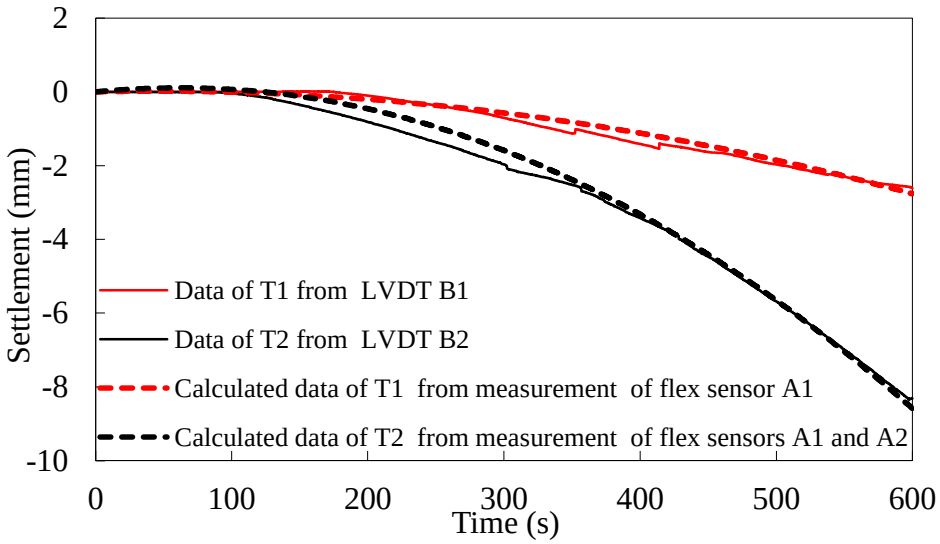

Figure 10 Calculated settlements of test points against time from LVDTs and flex sensors

6.3 Horizontal displacement and analysis

It should be noted here that the LVDT, B3, was misaligned caused by the occurred large soil deformation during the loading test. Hence, there were no accurate measurement data for B3. Figure 11 shows calculated tilt angle change against time of three flex sensors from the measurement data of flex sensors. It is clear that all tilt angles are varied within a range between -24° and 68°. The tilt angles of two flex sensors, A3 and A4, descended with time going, and the tilt angle of A3 decreased faster than that of A4. The tilt angle of A3 and A4 eventually approached the maximum tilt angles of around -24° and -14°, respectively. However, the tilt angle of A5 raise slowly at the first 200 s' period, and it increased linearly to around 68° from about 200 s to 400 s. Dramatically, the tilt angle of A5 ascended and descended smoothly and slowly to 62° eventually. The soil in present model was found to move in two opposite directions.

Therefore, flex sensors can be used to evaluate the underground movement conditions in terms of measurement data of flex sensors.

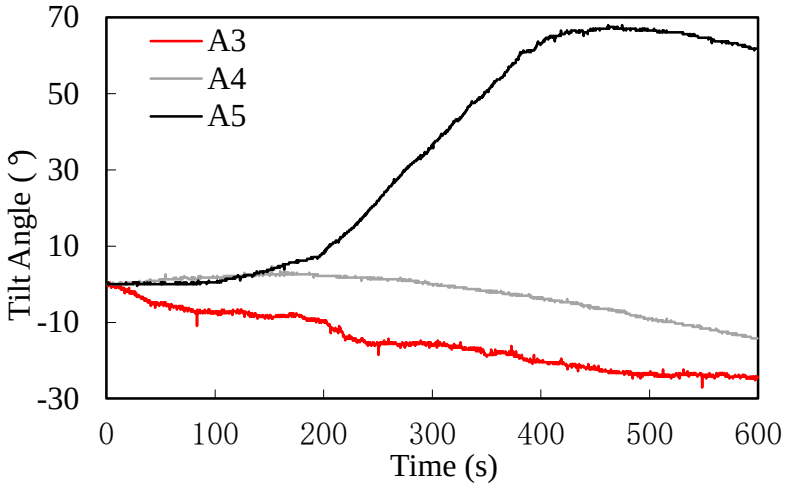

Figure 11 Tilt angle against time processed from measured data of five flex sensors

Assuming the horizontal displacement of test point (T3) calculated from the data measured from flex sensors as S_3, Figure 12 (a) and (b) give the exact sizes and positions of sections from flex sensors and LVDT and the schematic diagram of displacement calculation for these flex sensors, which is converted from Figure 7.

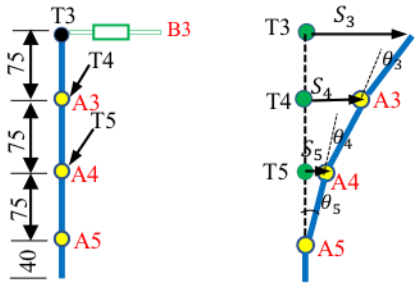

(a) (b)

Figure 12 (a) the initial sensing structure of flex sensors,
(b) A schematic diagram of horizontal displacement calculation (unit: mm)

According to Figure 12 (b), the tilt angles of the three flex sensors from bottom to the top of the flex sensors are θ_5, θ_4 and θ_3, respectively, and S_3, S_4, and S_5 represent horizontal displacements of the test points T3, T4 and T5, respectively. The horizontal displacements of T3, T4 and T5 measured from flex sensors can be calculated according to Eq. (1) and Figure 12.

Figure 13 shows the calculated horizontal displacements at three test points of T3, T4, and T5 respectively, against time from flex sensors. This soil deformation was initially small. According to two test points T4 (115 mm in slope depth) and T5 (190 mm in slope depth) was initially moving outside of the slope slowly and smoothly, but the initial horizontal soil displacement direction of test point T3 (190 mm in slope depth) was to the inside of the slope during the first 120 s. Such horizontal displacement

phenomenon could hardly be measured by traditional inclinometer. The maximum horizontal displacement in the slope inside direction of T3 was -11 mm at around 80 s. The cumulative horizontal displacements remain vary almost linearly against time with maximum displacement of around 210 mm, 135 mm, and 70 mm for the slope depth of 0 mm, 115 mm and 190 mm, respectively, from approximately 200 s to 420 s. Between around 200 s and 420 s, the horizontal displacements of all these three test points raised linearly against time, with at the rate of about 0.7 mm/s, 0.5 mm/s, and 0.3 mm/s for T3, T4, and T5, respectively. It is clear that the soil of smaller slope depth was in greater disturbance. The soil deformation increases with the rise of vertical load applied above the slope model. Since the upper slope soil was affected by the slope load the most, the horizontal displacement of T3 appeared the largest. After T3 reached the highest deformation, it started to drop quickly at the rate of around -0.2 mm/s. Besides, the horizontal soil displacement of T4 and T5 decreased slowly at the rate of around 0.08 mm/s and 0.02 mm/s, respectively. The speed of residual soil deformation of lower slope depth is quicker. This phenomenon was attributed to the soil's being compacted greater with the load increasing after the soil reached the maximum deformation, and the soil of lower slope depth hold more soil compaction change. As a result, flex sensors could be used to monitor the large deformation of slope.

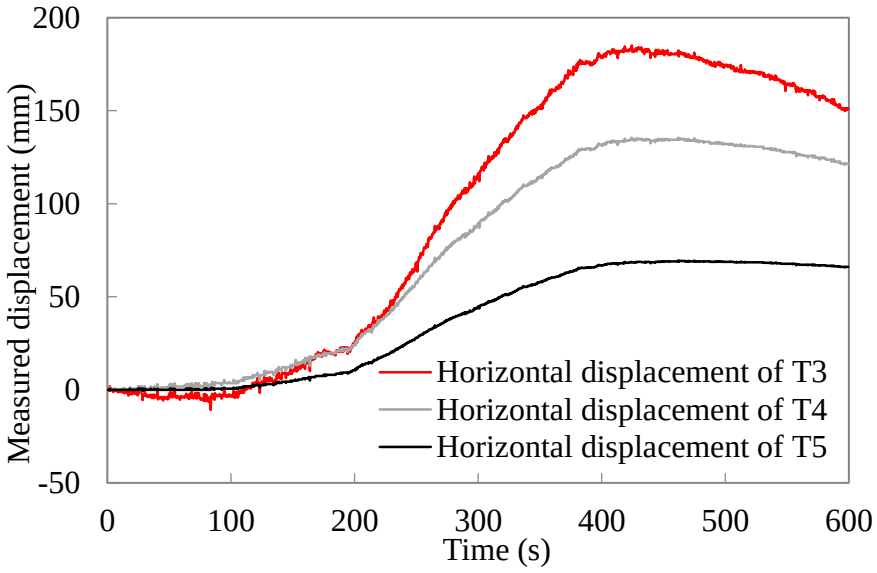

Figure 13 Calculated horizontal displacements of three test points against time from flex sensors

7. Conclusion

This paper proposed a wireless monitoring system of using flex sensors for measuring ground movement. Flex sensors of the wireless monitoring system were used to measure both soil settlement and horizontal ground movements of a sandy slope model due to continuous loading test in a laboratory, and the following conclusions can be drawn from the present study:

(a) A wireless monitoring system of using flex sensors was designed and fabricated combined with Bluetooth wireless transmission technology. This new system is characterized by high flexibility, large measurement range, ease of fabrication,

continuous output of real-time data, and quickly processing sensor data.

(b) Calibration tests indicate that flex sensors exhibit reliable measurement performance with a minimum resolution, sensitivity, and measurement range of 0.5°, 2.0~2.3 count/° and -30°~+70°, respectively. The calculated tilt angles in terms of physical parameters agree reasonably well with measured angles from angle gauges.

(c) A sandy slope model was built up and used to exam the measurement performance of FSS. Ground settlement of the sandy slope can be obtained from the measured tilt angles and calculated cumulative displacement from flex sensors. The measured data from flex sensors agree fairly well with the obtained displacement data from LVDTs with the maximum errors of less than 0.3mm and 0.5 mm, respectively when the maximum vertical displacements were approached.

(d) In terms of the horizontal ground movement monitoring, three flex sensors were mounted at three different sections along the sensing beams, forming an inclinometer. Horizontal ground displacement of the sandy slope can be observed from the measured tilt angles and calculated cumulative displacement from this FSS. The horizontal displacement calculated from the measurement data of flex sensors indicates the internal soil movement distribution of the slope model.

(e) It is noted that the flex sensor has limited measurement resolution, and hence it may be difficult for flex sensors to reflect small soil deformation. In this study, the authors carried out limited studies using FSS to monitor ground movement. More monitoring tests will be performed to exam the measurement performance of flex sensors in field, such as foundations, excavations, and different types of retaining walls.

Acknowledgement

The authors wish to thank the financial support from the National Key Research and Development Program of China under Grant 2018YFB2100901, in part by the National Natural Science Foundation of China (NSFC) under Project 41602352.

Reference

[1] L. M. Borges, N. Barroca, F. J. Velez, A. S. Lebres, Smart-clothing wireless flex sensor belt network for foetal health monitoring, International conference on pervasive computing. (2009) 1-4.

[2] P. Kumar, J. Verma, S. Prasad, Hand data glove: a wearable real-time device forhuman-computer interaction, Int. J. Adv. Sci. Technol. 43 (2012) 15–26.

[3] N. H. Adnan, K. Wan, S. Ab, S. Khadijah, H. Desa, M. Azri, et al., The development of a low cost data glove by using flexible bend sensor for resistive interfaces, The 2nd International Malaysia-Ireland Joint Symposiumon Engineering, Science and Business (IMiEJS2012) 2012 (2012) 579–587.

[4] S.K. Dixit, N.S. Shingi, Implementation of flex sensor and electronic compass for hand gesture based wireless automation of material, Int. J. Sci. Res. Publ. vol. 2 (December (12)) (2012) 2–4, ISSN 2250-3153.

[5] N. H. Adnan, K. Wan, A. B. Shahriman, M. H. Ali, M. Nasir Ayob, A. A. Aziz, Development of low cost GloveMAP based on fingertip bending tracking techniques for virtual interaction, Int. J. Mech. Mechatron. Eng. 12 (2012) 41–51.

[6] N. Tongrod, T. Kerdcharoen, N. Watthanawisuth, A. Tuantranont, A low-costdata-glove for Human computer interaction based on ink-jet printed sensor sand ZigBee networks, Int. Symp. Wearable Comput. 2010 (2010) 1–2.
[7] G. Saggio, F. Riillo, L. Sbernini, L. R. Qiuradamo,. Resistive flex sensors: a survey, Smart Materials and Structures, 25(1), (2015) 013001
[8] L. K. Simone, D. G. Kamper, Design considerations for a wearable monitor to measure finger posture, Journal of NeuroEngineering and Rehabilitation 2 (2005) 5.
[9] M. A. Saliba, F. Farrugia, A. Giordmaina, A compact glove input device to measure human hand, wrist and forearm joint positions for teleoperation applications, in: Proceedings of the IEEE/APS Int. Conf. on Mechatronics and Robotics, Aachen, Germany, September, 2004 (2004).
[10] S. Wise, W. Gardner, E. Sabelman, E. Valainis, Y. Wong, K. Glass, et al., Evaluation of a fiber optic glove for semi-automated goniometric measurements, Journal of Rehabilitation Research and Development 27 (4) (1990) 411–424.
[11] R. Gentner, J. Classen, Development and evaluation of a low-cost sensor glove for assessment of human finger movements in neurophysiological settings, Journal of Neuroscience Methods 178 (2009) 138–147.
[12] F. Lorussi, W. Rocchia, E.P. Scilingo, A. Tognetti, D. De Rossi, Wearable, redundant fabric-based sensor arrays for reconstruction of body segment posture, IEEE Sensors Journal 4 (6) (2004) 807–818.
[13] T. Someyal, T. Sakurai, T. Sekitanil, Future prospects of flexible, large-area sensors and actuators with organic transistor, in: IEEE International Electron Devices Meeting, 2005, IEDM Technical Digest., 5 December, 2005 (2005).
[14] A. Raut, V., Singh, V., Rajput, R., Mahale, Hand sign interpreter, (2012)19–25.
[15] A.S. Ghotkar, R. Khatal, S. Khupase, S. Asati, M. Hadap, Hand gesture recognition for indian sign language, Computer Communication and Informatics (ICCCI). 2012 International Conference on. IEEE 4 (2012) 1–4.
[16] G. Saggio, A novel array of flex sensors for a goniometric glove, Sens. Actuators, A Phys. 205 (2014) 119–125.
[17] S. Bakhshi, M. H. Mahoor, Development of a wearable sensor system formeasuring body joint flexion, Proc. -Int. Conf. Body Sens. Netw., BSN 2011(2011) 35–40.
[18] G. Saggio, L. Bianchi, S. Castelli, M. Santucci, M. Fraziano, A. Desideri, In vitro analysis of pyrogenicity and cytotoxicity profiles of flex sensors to be used to sense human joint postures, Sensors 14 (2014) 11672–11681.
[19] P. Walters, D. McGoran, Digital fabrication of smart structures and mechanisms—creative applications in art and design, International Conference on Digital Printing Technologies and Digital Fabrication 2011.(27), USA: The Society for Imaging Science and Technology. (2011) 185–188.
[20] D. Hanafi, Wireless surface electrical stimulation with knee joint angle measurement system using gyroscope and flex bend sensors, Journal of

Biosensors and Bioelectronics (2013).
[21] M. Anwar, M. A. F. M. Noor, W. M. F. W. M. Fadzil, L. H. Omar, M. S. Ramli, Prototype development of a simple Hearing Impaired Sign Language Translator Glove using Flex sensor, JSET. 3 (2016) 88-91.
[22] G. Saggio, Mechanical model of flex sensors used to sense finger movements. Sensors and Actuators A: Physical 185 (2012) 53-58.
[23] G. Ponraj, H. Ren, Sensor Fusion of Leap Motion Controller and Flex sensors Using Kalman Filter for Human Finger Tracking, IEEE Sensors Journal 18. 5 (2018) 2042-2049.
[24] S. Uhlemann, A. Smith, J. E. Chambers, N. Dixon, T. Dijkstra, E. Haslam, P. I. Meldrum, A. Merritt, D. A. Gunn, J. Mackay, Assessment of ground-based monitoring techniques applied to landslide investigations, Geomorphology. (2016) 438-451.
[25] J. Li, R. Correia, E. Chehura, S. Staines, S. W. James, R. P. Tatam, A fibre Bragg grating-based inclinometer system for ground movement measurement, Proc. SPIE 7653. Fourth European Workshop on Optical Fibre Sensors. 765314 (2010).
[26] J. S. Bajić, D. Z. Stupar, A. Jože, M. P. Slankamenac, M. Jelić, and M. B. Živanov, A simple fibre optic inclination sensor based on the refraction of light, Physica scripta, vol. 2012 (2012) 014024.
[27] Y. T. Ho, A. B. Huang, and J. T. Lee, Development of a fibre Bragg grating sensored ground movement monitoring system, Measurement Science and Technology, vol. 17. (2006) 1733.
[28] C. Hong, Y. Zhang, Z. Lu, Z. Yin, A FBG Tilt Sensor Fabricated Using 3D Printing Technique for Monitoring Ground Movement, IEEE Sensors Journal 19.15. (2019) 6392-6399.
[29] B. J. Peng, Y. Zhao, Y. Zhao, and J. Yang, "Tilt sensor with FBG technology and matched FBG demodulating method," Sensors Journal, IEEE. vol. 6. (2006) 63-66.
[30] S. C. Kang, S. Y. Kim, S. B. Lee, S. W. Kwon, S. S. Choi, and B. Lee, Temperature-independent strain sensor system using a tilted fiber Bragg grating demodulator, Photonics Technology Letters. IEEE. vol. 10. (1998) 1461- 1463.
[31] Y. Zheng, D. Huang, and L. Shi, A new deflection solution and application of a fiber Bragg grating-based inclinometer for monitoring internal displacements in slopes, Measurement Science and Technology. vol. 29. (2018) 055008.